CHAPTER - VI

HEAT FLOW PROCESSES IN THE POSITIVE COLUMN OF A LOW PRESSURE MERCURY ARC.

CHAPTER - VI

HEAT FLOW PROCESSES IN THE POSITIVE COLUMN OF A LOW PRESSURE MERCURY ARC.

INTRODUCTION

The heat transport properties of confined electric arc plasma (i.e. the electric arc burning in a tube with cold walls) have been investigated by a number of investigators during the past few decades (Maecker, 1960; Ulenbusch, 1964; Emmons and Land, 1962, etc.). Emmons and Land (1962) measured the thermal conductivity of argon and helium between 5000°K to 10000°K. They assumed Elenbaas-Heller heat balance equation (Elenbaas, 1951) with the inclusion of a radiation term. The model, as it has been treated, rests upon an equation expressing simply the balance of three terms :

(1) Heat generation by Joule Effect,
(2) Heat transfer by thermal conduction,
(3) Heat transfer by radiation.

However, they were able to show that the radiation loss was a few percent of the total loss and in their report the radiation effect had been lumped with some effective thermal conductivity. In general, the electrical conductivity assumes a radial distribution within the arc tube but for simplification they assumed the "Channel Model" (Hoyaux, 1968) for the electrical conductivity distribution within the arc.

In a later paper Emmons (1967) studied the heat transport of high temperature (7500°K to 13750°K), high pressure argon and helium gas using confined electric arc and tackled the problem very rigorously treating the radiation loss in an adequate manner.

Knopp and Cambel (1966) measured the radial temperature distribution within a cylindrically symmetric argon plasma column by spectroscopic method. Using the measured temperature profiles and theoretically calculated radiated power, the thermal conductivity of argon was determined for the temperature range 8500°K to 12000°K.

Most of the experiments aimed at determining the transport properties of noble gases at very high temperatures. At those temperatures thermal ionization prevails and radial distribution of electrical conductivity and thermal conductivity could be calculated using Saha's equation knowing the radial distribution of the gas temperature T. In those cases all the constituents of the gas were considered to be in thermal equilibrium. Goldstein and Sekiguchi (1958) have done elegant experiments employing microwave technique to determine thermal conductivity of a decaying glow discharge plasma where the plasma constituents were also in thermal equilibrium.

It is worthwhile to mention at this stage that no reference in the literature is available where the process of heat flow in a confined low pressure arc (where the electrons are far from being in thermal equilibrium with the heavier constituents) has been adequately studied. The work presented in this Chapter devotes to study semi-emperically the heat flow processes occurring within a low pressure mercury arc plasma.

In a previous Chapter and also in a paper by the present author and others (Ghosal et al 1978) it has been shown that when an arc is formed within a tube, the current density is not uniform throughout the cross-section but is maximum at the axis and minimum at the periphery. This phenomenon gives rise to selective self-heating at the axis of the arc plasma. The arc continuously absorbs power from the source and gives it away to the surroundings. One might therefore be tempted to consider that the mechanism of selective self-heating might be employed to determine thermal conductivity of the plasma. There are justifications in neglecting the effect of radiation and convection in the case of low temperature arcs* but nevertheless it is worthwhile

---

* It may be seen in our discussion that even ignoring the effect of radiation and convection the obtained value of ion-neutral atom collision cross-section falls at the higher side. If any significant contribution of those terms are incorporated the calculations would lead to absurd results. Thus we may assume that the radiation and convection effects are fairly small if not insignificant.

to mention that in this case the process of heat flow requires close observations. In a weakly ionised plasma both the electronic and molecular contributions to thermal conductivity are to be considered. One might predominate substantially over the other depending on the electron temperature, temperature gradients (electron temperature and gas temperature etc.). There might be present another mechanism of heat flow other than thermal conduction, radiation and convection, which arises due to the fact that electron density distribution within the arc may cause diffusion and energy might be carried away by the electrons. In contrast to the case of high pressure arc this mechanism of heat flow might play a significant role in case of low pressure arcs.

The purpose of the following article is to present the study of these processes and to compare them in the present experimental conditions. It will also be shown that this study yields valuable information about electron-atom collision cross-section at very low electron energies.

THEORETICAL CONSIDERATION

In the previous Chapters (Chapter IV and V and also Ghosal et al 1978) it has been reported that the present author has studied the radial structure of electrical conductivity of a mercury arc plasma in an arc tube by a new radio frequency probe technique. There it has been shown that the radial electrical conductivity distribution function can well be represented by the formula

$$\sigma(r) = \sigma_0 \left[1 - \left(\frac{r}{R}\right)^2 \right]^n \qquad .. (6.1)$$

where r represents the radial position, R the radius of the tube and σ_0, the conductivity at the axis. The experimentally determined term 'n' is found to be dependent on discharge currents. As indicated in the previous section this radial distribution of electrical conductivity gives rise to a distribution of the rate of heating inside the plasma cylinder defined by the radii r and r + dr. The rate of heating per unit length $d\dot{Q}_0$ within the annular space can be represented as

$$d\dot{Q}_0 \propto \Sigma(r)$$

where $\Sigma(r)$ is the electrical conductance of the annular plasma cylinder considered and is given by

$$\Sigma(r) = 2\pi r \sigma(r) \, dr$$

Thus we can write,

$$d\dot{Q}_0 = c \, r \, \sigma(r) \, dr$$

where C is a constant. The rate of heating inside the plasma cylinder of radius r is given by

$$\int_0^r c \, r \, \sigma(r) \, dr = c \, F(r) \quad , \ (\text{say}) \qquad .. (6.2)$$

Now let us turn our attention to the Boltzmann transport equation for electrons in absence of magnetic field,

$$\frac{\partial f_e(\vec{x},\vec{v},t)}{\partial t} + \vec{v}\cdot\frac{\partial f_e(\vec{x},\vec{v},t)}{\partial \vec{x}} - \frac{e}{m_e}\vec{E}\cdot\frac{\partial f_e(\vec{x},\vec{v},t)}{\partial \vec{v}} = -\nu_{me} f_{e1}$$

where f_e is the electron distribution function, $\vec{E} = \vec{E}(\vec{x},t)$ is the electric field, ν_{me} is the effective electron-atom collision frequency and f_{e1} is the perturbation in the equilibrium distribution function. At equilibrium, considering one-dimensional case and taking first order approximation (assuming f_{e1} is very small in comparison to the equilibrium distribution function f_{eo}) and thereby linearising one gets,

$$v_z \frac{\partial f_{eo}}{\partial z} - \frac{eE_z}{m_e}\frac{\partial f_{eo}}{\partial v_z} = -\nu_{me} f_{e1} \quad \text{..} \quad (6.3)$$

where E_z is the field produced in the z-direction due to diffusion of charged particles, where the equilibrium function is given by

$$f_{eo} = \phi(z)\left(\frac{m_e}{2\pi k T_e}\right)^{3/2} \cdot e^{-\frac{m_e v^2}{2kT_e}} \quad \text{..} \quad (6.4)$$

where $\phi(z)$ is related to the electron density by

$$n(z) = n_o\,\phi(z) = n_o\left[1 - \left(\frac{r}{R}\right)^2\right]^n \quad \text{..} \quad (6.5)$$

(Since we are interested in calculating the heat flux we intentionally omit the contribution of the supply field because the net heat flux within a given cylindrical volume due to the presence of this field will be zero).

Now from equation (6.3) f_{e1} can be determined if proper value of E_z is substituted. Assuming electron and ion density to be approximately equal i.e. $n_e \simeq n_i = n(z)$ and there is no net accumulation of charge in the plasma, we get (see appendix 6A),

$$-\frac{D_i}{n}\frac{dn(z)}{dz} + \mu_i E_z = -\frac{D_e}{n}\frac{dn(z)}{dz} - \mu_e E_z \qquad \text{.. (6.6)}$$

where D_e, D_i and μ_e, μ_i are the diffusion coefficients and mobilities of electrons and ions respectively

or,

$$E_z = -\frac{1}{\Phi(z)} \cdot \frac{D_e - D_i}{\mu_e + \mu_i} \frac{d\Phi(z)}{dz} \qquad \text{.. (6.7)}$$

Substituting equation (6.7) in equation (6.3)

$$v_z \frac{\partial f_{eo}}{\partial z} + \frac{e(D_e - D_i)}{m_e(\mu_e + \mu_i)} \cdot \frac{1}{\Phi(z)} \cdot \frac{d\Phi(z)}{dz} \frac{\partial f_{eo}}{\partial v_z} = -\nu_{me} f_{e1}$$

or, $$f_{e1} = -\frac{v_z}{\nu_{me}}\frac{\partial f_{eo}}{\partial z} - \frac{e}{\nu_{me} m_e}\frac{D_e - D_i}{\mu_e + \mu_i} \cdot \frac{1}{\Phi(z)} \cdot \frac{d\Phi(z)}{dz} \cdot \frac{\partial f_{eo}}{\partial v_z} \qquad \text{.. (6.8)}$$

Recalling,

$$f_{eo} = \phi(z)\left(\frac{m_e}{2\pi k T_e}\right)^{3/2} \cdot e^{-\frac{m_e v^2}{2kT_e}},$$

$$\frac{\partial f_{eo}}{\partial z} = \phi(z)\frac{\partial}{\partial T_e}\left[\left(\frac{a}{T_e}\right)^{3/2} \cdot e^{-b/T_e}\right]\frac{\partial T_e}{\partial z} + \left(\frac{a}{T_e}\right)^{3/2} \cdot e^{-b/T_e} \cdot \frac{\partial \phi(z)}{\partial z} \quad .. \quad (6.9)$$

where $a = \left(\frac{m_e}{2\pi k}\right)^{3/2}$ and $b = \frac{m_e v^2}{2k}$ .. (6.10)

and also $$\frac{\partial f_{eo}}{\partial v_z} = 2\,\phi(z)\,A B\, v_z\, a^{-Bv^2} \quad .. \quad (6.11)$$

where $A = \left(\frac{m_e}{2\pi k T_e}\right)^{3/2}$ & $B = \frac{m_e}{2kT_e}$ .. (6.11a)

Writing 1st. term and 2nd. term of R.H.S. of equation (6.8) to be f'_{e1} and f''_{e1} respectively, one obtains,

$$f_e = f_{eo} + f'_{e1} + f''_{e1} \quad .. \quad (6.12)$$

Thus the electron contribution of heat flux can be obtained as,

$$H_e = \iiint_{-\infty}^{+\infty} n_0 \left(\tfrac{1}{2} m_e v^2\right) v_z f_e \, dv_x \, dv_y \, dv_z$$

$$= \iiint_{-\infty}^{+\infty} n_0 \left(\tfrac{1}{2} m_e v^2\right) v_z \left(f_{e0} + f_{e1}' + f_{e1}''\right) dv_x \, dv_y \, dv_z$$

$$= \iiint_{-\infty}^{+\infty} n_0 \left(\tfrac{1}{2} m_e v^2\right) v_z f_{e1}' \, dv_x \, dv_y \, dv_z + \iiint_{-\infty}^{+\infty} n_0 \left(\tfrac{1}{2} m_e v^2\right) v_z f_{e1}'' \, dv_x \, dv_y \, dv_z$$

$$= H_1 + H_2 \quad \text{(say)} \qquad .. \quad (6.13)$$

(Since $\iiint_{-\infty}^{+\infty} n_0 \left(\tfrac{1}{2} m_e v^2\right) v_z f_{e0} \, dv_x \, dv_y \, dv_z$ vanishes)

(See Appendix 6B).

The terms H_1 and H_2, i.e. the 1st. and 2nd. integrals of equation (6.13) can be obtained by using equations (6.8), (6.9), (6.10), (6.11), (6.11a) and (6.13).

$$H_1 = -\frac{5}{2} \frac{n_0 \phi(z) k^2}{m_e \nu_{me}} T_e \frac{dT_e}{dz} - \frac{5}{2} \frac{n_0}{m_e} \cdot \frac{k^2}{\nu_{me}} T_e^2 \frac{d\phi(z)}{dz} \qquad .. \quad (6.14)$$

$$= -K_e \frac{dT_e}{dz} - \frac{5}{2} D_e \frac{d\phi(z)}{dz} \cdot n_0 k T_e \qquad .. \quad (6.15)$$

where $K_e = \frac{5}{2} \frac{n_0 \phi(z) k^2}{m_e \nu_{me}} \cdot T_e$ is the electronic thermal conductivity of the plasma and $D_e = \frac{k T_e}{m_e \nu_{me}}$ is the diffusion coefficient of electrons.

And $$H_2 = \frac{5}{2} n_0 k T_e \mu_e \frac{D_e - D_i}{\mu_e + \mu_i} \cdot \frac{d\phi(z)}{dz} \qquad .. \quad (6.16)$$

where the electron mobility $\mu_e = e/m_e \nu_{me}$

Now since $T_e/m_e \gg T_i/m_i$, we can write $D_e - D_i \simeq D_e$

and since $\mu_e \gg \mu_i$, we can write to a 1st. approximation,

$$(\mu_e + \mu_i)^{-1} = \frac{1}{\mu_e}\left(1 - \frac{\mu_i}{\mu_e}\right)$$

Thus equation (6.16) becomes,

$$H_2 = \frac{5}{2} n_0 k T_e D_e \frac{d\phi(z)}{dz} - \frac{5}{2} n_0 k T_e \cdot \frac{\mu_i}{\mu_e} \cdot D_e \cdot \frac{d\phi(z)}{dz} \qquad .. \quad (6.17)$$

Hence $$H_e = -K_e \frac{dT_e}{dz} - \frac{5}{2} n_0 k T_e \frac{\mu_i}{\mu_e} \cdot D_e \qquad .. \quad (6.18)$$

or $$H_e = -k_e \frac{dT_e}{dz} - \frac{5}{2} n_0 k T_e D_A \frac{d\phi(z)}{dz} \qquad .. \quad (6.19)$$

where $D_A = \frac{\mu_i}{\mu_e} \cdot D_e$ is the approximate ambipolar diffusion coefficient. The second term of the R.H.S. of equation (6.19) can be interpreted in the following way :

The flux of electrons Γ_e executing ambipolar diffusion is given by,

$$\Gamma_e = -D_A \frac{dn(z)}{dz} = -D_A n_0 \frac{d\phi(z)}{dz}$$

Therefore, energy flux carried away by these electrons will be the average kinetic energy multiplied by Γ_e .

Again, average K.E. $\propto kT_e$

Thus heat flux will be,

$$H_{amb} = -\text{Const.}\ k T_e\, n_o D_A \frac{d\,\phi(z)}{d\,z}$$

Hence, the 2nd. term on the R.H.S. of equation (6.19) is the heat flux due to the ambipolar diffusion of electrons.

The total heat flux, however, will contain other terms H_i and H_n for the ion species and the neutral particle species respectively. H_i can be neglected in comparison to H_e since ion temperature is very small in comparison to that of electrons.

Thus $$\mathcal{H} = H_e + H_n$$

$$= -\frac{5}{2}\,\frac{n_o}{m_e}\cdot\frac{k^2}{\nu_{me}}\cdot\phi(z)\cdot T_e\frac{dT_e}{dz} - \frac{5}{2}\,n_o k T_e\frac{\mu_i}{\mu_e}D_e\,\frac{d\,\phi(z)}{d\,z} - K_n\frac{dT_n}{dz}$$

where K_n is the thermal conductivity for the mercury gas.

Assuming cylindrical symmetry Z can be replaced by the radial variable r.

Hence

$$H = -\frac{5}{2}\,\frac{n_o}{m_e}\cdot\frac{k^2}{\nu_{me}}\,\phi(r)\,T_e\frac{dT_e}{dr} - \frac{5}{2}\,n_o k T_e\frac{\mu_i}{\mu_e}\cdot D_e\frac{d\phi(r)}{dr} - K_n\frac{dT_n}{dr}$$

The heat flow across the plasma cylinder of unit length of radius r is given by,

$$C F(r) = 2\pi r\left[-\frac{5}{2}\,\frac{n_o}{m_e}\cdot\frac{k^2}{\nu_{me}}\,\phi(r)\,T_e\,\frac{dT_e}{dr} - \frac{5}{2}\,n_o k T_e\,\frac{\mu_i}{\mu_e}\,D_e\,\frac{d\phi(r)}{dr} - K_n\,\frac{dT_n}{dr}\right]$$

or, assuming $T_e(r) = \bar{T}_e$, i.e. some suitable average value of electron temperature within the plasma column,

$$C\int_0^R \frac{F(r)\,dr}{r} = 2\pi\left[\frac{5}{2}\,\frac{n_o}{m_e}\,\frac{k^2\,\overline{\phi(r)}}{\nu_{me}}\cdot\bar{T}_e\left(T_{eo}-T_{ew}\right) + \frac{5}{2}\,n_o k\bar{T}_e\,\frac{\mu_i}{\mu_e}\,D_e(\phi_o-\phi_w) + K_n\left(T_{no}-T_{nw}\right)\right] \quad .. \quad (6.20),$$

where the suffices o and W refer to the values of the relevant quantities at the axis and at the wall respectively. Again, let us turn our attention to the equation (6.2),

$$\int_0^R c\,r\,\sigma(r)\,dr = C\,F(R) = \dot{Q}_0 \quad (\text{say})$$

where $\dot{Q}_0$ is the total rate of heating inside the plasma column of unit length. Thus,

$$C = \dot{Q}_0 \,/\, F(R) \qquad (6.2a)$$

Now using equation (6.2a) we have from equation (6.20)

$$\Lambda \dot{Q}_0 = 2\pi\left[\alpha\,\overline{\phi(r)}\,T_e\left(T_{eo}-T_{ew}\right)+\beta\left(\phi_0-\phi_w\right)+K_n\left(T_{no}-T_{nw}\right)\right] \quad (6.21)$$

(henceforth omitting the bar (-) sign over T_e)

where

$$\Lambda = \int_0^R \frac{F(r)}{r}\,dr \Big/ F(R) \quad (6.22)$$

(See Appendix 6-C).

With

$$\alpha = \frac{5}{2}\,\frac{n_0}{m_e}\,\frac{k^2}{\nu_{me}} \quad (6.23)$$

and

$$\beta = \frac{5}{2}\,n_0 k T_e \frac{\mu_i}{\mu_e} D_e = \alpha \frac{\mu_i}{\mu_e} T_e^2 \quad (6.24)$$

The electrical conductivity at the axis of the plasma column is given by the relation,

$$\sigma_0 = \frac{n_0 e^2}{m_e \nu_{me}} \quad (6.25)$$

Thus,

$$\alpha = \frac{5}{2}\,\frac{\sigma_0 k^2}{e^2} \quad (6.26)$$

and

$$\beta = \frac{5}{2}\,\frac{\sigma_0 k^2}{e^2}\cdot\frac{\mu_i}{\mu_0}\cdot T_e^2 \quad (6.27)$$

Assuming $\overline{\phi(r)} \simeq 1/2$ to a 1st. approximation, we can rewrite equation (6.21) in the form

$$\Lambda \dot{Q}_o = \frac{5}{2}\pi \frac{k^2}{e^2} \sigma_o T_e \left(T_{eo} - T_{ew}\right) + 5\pi \frac{\mu_i}{\mu_e} \cdot \frac{k^2}{e^2} \sigma_o T_e^2 \left(\phi_o - \phi_w\right) + 2\pi K_n \left(T_{no} - T_{nw}\right) \quad .. \quad (6.28)$$

The quantity $T_{no} - T_{nw}$ can be known experimentally by using thermometers (vide experimental arrangement). If the longitudinal electric field of the plasma is assumed to be uniform throughout the cross-section of the plasma the quantity $(T_e - T_n)$ becomes a constant parameter within it.*

Thus one can assume $T_{eo} - T_{ew} = T_{no} - T_{nw}$.

Hence equation (6.28) takes the form,

$$\dot{Q}_o = \frac{5}{2}\pi \frac{k^2}{e} \frac{\sigma_o}{\Lambda} T_e \left(T_{no} - T_{nw}\right) + 5\pi \frac{\mu_i}{\mu_e} \cdot \frac{k^2}{e^2} \cdot \frac{\sigma_o}{\Lambda} T_e^2 + 2\pi \frac{K_n}{\Lambda} \left(T_{no} - T_{nw}\right) \quad .. \quad (6.29)$$

---

* This is true since electron temperature T_e is, in the constant collision approximation, related to the gas temperature T_g and the applied electric field E as follows :

$$T_e = T_g + M/3k \left(eE/m\nu_m\right)^2 \quad \text{(Persson, 1961)}$$

where M and m are the masses of the neutral gas particle and the electron, respectively, while k is the Boltzmann constant.

where we have put $\phi_0 = 1$ and $\phi_w = 0$ according to the proposed distribution function,

The quantity $\Lambda = \dfrac{\int_0^R \dfrac{\int_0^r r\,\sigma(r)\,dr}{r}\,dr}{\int_0^R r\,\sigma(r)\,dr}$

can be determined if $\sigma(r)$ is known beforehand.

The equation (6.29) can also be written as

$$\dot{Q}_0 = \dot{Q}_K + \dot{Q}_D + \dot{Q}_n \quad .. \quad (6.30)$$

where

$$\dot{Q}_K = \frac{5}{2}\pi \frac{k^2}{e^2} \frac{\sigma_0}{\Lambda} T_e \left(T_{n0} - T_{nw}\right) \quad .. \quad (6.31)$$

is the rate of heat flow from the plasma per unit length to the wall due to electronic thermal conductivity;

$$\dot{Q}_D = 5\pi \frac{\mu_i}{\mu_e} \frac{k^2}{e^2} \frac{\sigma_0}{\Lambda} T_e^2 \quad .. \quad (6.32)$$

is the heat flow rate due to ambipolar diffusion of electrons;

and

$$\dot{Q}_n = 2\pi \frac{K_n}{\Lambda} \left(T_{n0} - T_{nw}\right) \quad .. \quad (.6.33)$$

is the heat flow rate due to thermal conduction of neutral particles.

EXPERIMENTAL ARRANGEMENT AND RESULTS

The schematic experimental arrangement is shown in figure (6.1). The apparatus consists of a mercury arc tube (length: 31 cms., internal dia.: 1.5 cms.; external dia.: 1.9 cms.) with the usual D.C. source, rheostat (R), ammeter(A) arrangements. The arc tube has got some special constructional features. A condenser of length 20 cms. is fitted along the mid-portion of the tube to facilitate the flow of water around the positive column of the mercury arc. The temperature of the outflowing water can be measured with an ordinary mercury thermemeter fitted with the condenser. A thin glass capsule containing a small platinum-wire coil is placed at the axis of the tube. The coil having its leads outside the tube serves the purpose of a platinum resistance thermometer. The other accessories which are required to record the resistance of the thermometer at different temperatures are not shown in the figure. There is also a double-probe arrangement to measure the voltage across the positive column and one of the probes may be utilised to measure the electron temperature.

The experimental procedure is quite straight-forward. The platinum resistance thermometer is first calibrated and water is made to flow through the condenser. The arc is then drawn along the tube. Some time is allowed to pass to achieve the thermal equilibrium of the platinum thermometer with the mercury vapour at the axis. The temperature of the platinum thermometer reads T_{no}, the temperature at the axis. The mercury thermometer reads the temperature θ of the outflowing water. Due to the finite conductivity of glass, this θ is not the actual peripheral temperature of the plasma. Knowing the thickness and the conductivity (K_g) of the glass of the tube, the actual peripheral temperature T_{nw} is calculated. The experiment is repeated for different discharge currents. In each case the rate of supply of heat $\dot{Q}_o$ is calculated by knowing the discharge current and the voltage across the plasma column under study. The experimental results are given below in tabular form (Table 6.1) which is self-explanatory. The $\dot{Q}_o$'s have been calculated from the measured values of E and I.

DISCUSSION

In Chapter IV (and also Ghosal et al, 1978) the electrical conductivity distribution function was determined for an arc plasma in an arc tube having the same dimension as the present one and the discharge conditions also were the same. Hence here also we assume the same set of distribution functions at 2.3 amps., 3.1 amps. and 4.0 amps. of discharge currents. The value of the quantity

$$\Lambda = \frac{\int_0^R \frac{\int_0^r r\,\sigma(r)\,dr}{r}\,dr}{\int_0^R r\,\sigma(r)\,dr}$$

where $\sigma(r) = \sigma_0\left[1 - \left(\frac{r}{R}\right)^2\right]^n$ the parameter n being dependent on discharge currents, may be solved numerically. Given below in Table 6.2 the values of σ_0, n and Λ at different discharge currents.

TABLE - 6.1

Experimental Results

Discharge current in Amps. (I)	Longitudinal electric field in volt/cm. (E)	$\dot{Q}_o$ in ergs/cm.sec.	Temperature at the axis in °C (T_{no})	Temperature of the outflowing water in °C (θ)	Actual gas temp. at the periphery in °C (T_{nw})	$T_{no}-T_{nw}$ in °C	Electron temp. in °K (Probe meas.) (T_e)	Average gas temp. $\bar{T}_g = \bar{T}_i$ in °K.
2.3	0.685	1.57	102.8	37.5	41.3	61.5	1.76×10^4	345.10
3.1	0.472	1.46	105.5	38.0	41.6	63.9	3.50×10^3	346.55
4.0	0.425	1.70	111.4	39.0	43.1	68.3	3.23×10^3	350.30

TABLE - 6.2

Values of σ_o, n and Λ for different discharge currents

Discharge current in Amp. (I)	σ_o (mhos/cm.)	n	Λ
2.3	6.26	2.293	0.8800
3.1	18.05	3.859	1.0561
4.0	26.55	3.984	1.0676

In table 6.3 the values of quantities $\dot{Q}_o$, $\dot{Q}_k$ and $\dot{Q}_n$ (in Joules/cm.sec.) are inserted for three different discharge currents (2.3 amps., 3.1 amps. and 4.0 amps.). To obtain $\dot{Q}_n$, the value of K_n has been taken to be 1.5 x 10^5 cals/cm.sec. obtained from the kinetic theory data for mercury gas.

It may clearly be seen that there is little contribution of $\dot{Q}_n$, i.e. the heat flow due to neutral particles, to the total heat flow rate. It is also observed that heat flow due to electronic thermal conductivity is below 30% of the total flow rate for 2.3A discharge current and at lower electron temperatures the contribution of electronic thermal conductivity term decreases and in the present situation heat is mainly carried away to the wall by electrons due to ambipolar diffusion.

The column for $\dot{Q}_D$ has been obtained from the equation (6.30) and $\dot{Q}_n$ has been neglected.

Now equation (6.32) may be utilised to obtain the mobility ratio μ_i/μ_e or expressing this ratio in terms of the mean free path ratio λ_i/λ_e one obtains from equation (6.32),

$$\dot{Q}_D = 5\pi\sqrt{\frac{m_e}{m_i}}\;\frac{k^2}{e^2}\;\frac{\sigma_0}{\Lambda}\;\frac{T_e^{5/2}}{T_i^{1/2}}\cdot\frac{\lambda_i}{\lambda_e} \quad .. \quad (6.34)$$

where T_i is the average ion temperature.

Here we shall make another assumption :

$T_i \simeq \bar{T}_n$ where $\bar{T}_n$ is the average gas temperature, and so we can rewrite equation (6.34) as

$$\dot{Q}_D = 5\pi\sqrt{\frac{m_e}{m_i}}\;\frac{k^2}{e^2}\;\frac{\sigma_0}{\Lambda}\;\frac{T_e^{5/2}}{T_i^{1/2}}\;\frac{q_e}{q_i}$$

where q_e/q_i is the ratio of the electron-atom to ion-atom cross-section. In the 7th. column (Table 6.3) the obtained values of q_e/q_i are inserted. Since in the present experiment the ion energy remains fairly constant, we can assume q_i to be a constant quantity. Thus it may be seen that there is a remarkable increase of electron-atom collision cross-section as the electron temperature falls to a value of the order of 3×10^3 °K (at discharge currents 3.1 and 4.0 amps.) from its value 1.76×10^4 °K at 2.3 amps. discharge current.

In the 9th. column the electron energies are inserted in electron volt. The electron-Hg. atom collision cross-section can be estimated from Brode's measurements (Brode, 1933) and(Massey, 1969). But for energies <1 ev. the q_e values are not well known (Von Engel, 1964). However, q_e can be obtained from Brode's curve for electron energy 2.97 ev. This is found to be 6.226×10^{-15} sq. cm. Utilising this value of q_e the value of q_i is obtained to be 16.78×10^{-15} sq. cm. This value shows quite an order of magnitude agreement with the mercury atom-atom collision cross-section, which is $4\pi\sqrt{2}\,r^2 = 8.059 \times 10^{-15}$ sq. cm., where r is the radius of the mercury atom. This agreement not only justifies our previous arguments but also the obtained value of q_i can be utilized to determine the values of q_e at two different electron energies below 1 ev., thus enabling us to extend Brode's curve in the lower electron energies (Table 6.4). Our results also corroborates with the results obtained by Margenau and Adler (1950) who predicted an occurrence of maxima in the region of lower electron energies from where Brode's measurements begin. The obtained high values of electron-atom collision cross-sections at lower electron energies also explains the sudden fall of electron temperature at higher discharge currents, since as the current is increased the vapour pressure of Hg. increases, and thereby lowers the electron energy to some extent. These low energy electrons again suffer greater number of collisions due to sharp rise of q_e at lower electron energies, thereby lowering the electron energy again and the process continues until the equilibrium is reached.

TABLE - 6.3

I (in amp.)	$\dot{Q}_o$ (ergs/cm. sec.)	$\dot{Q}_K$ (ergs/cm. sec.)	$\dot{Q}_D$ (ergs/cm. sec.)	$\dot{Q}_n$ (ergs/cm.sec.)	$\dot{Q}_K / \dot{Q}_D$	q_e / q_i	T_e in ^oK	Electron energy in ev.
2.3	1.58	0.45	1.12	2.76×10^{-2}	0.28	0.371	1.76×10^4	2.97
3.1	1.46	0.22	1.24	2.40×10^{-2}	0.15	9.723	3.50×10^3	0.45
4.0	1.70	0.32	1.38	2.53×10^{-2}	0.19	9.149	3.23×10^3	0.42

TABLE - 6.4

Discharge current (amp.) (I)	Electron energy (ev.)	q_e (sq. cm.)
2.3	2.97	6.23×10^{-15}
3.1	0.45	1.63×10^{-13}
4.0	0.41	1.53×10^{-13}

APPENDIX 6A

Arriving at Equation (6.6)

Let us suppose that at an instant of time the positive ions and electrons assume the same arbitrary spatial density distribution within the plasma. In some later instant of time the distribution is expected to be changed due to unequal diffusion velocity for the lighter and heavier ions of the plasma. As the density distribution function for the two species go on to differ, an electric field is set up which would retard the electrons and enhance the positive ion motion. When the equilibrium is reached the flow of both the positive ions and the electrons becomes equal. The flow of ions is now governed by the combined effect of diffusion and drift due to the space charge field produced. The particle flux of the ion type α thus may be given by

$$\Gamma_\alpha = - D_\alpha \vec{\nabla} n_a + \mu_\alpha \vec{E_s} n_a$$

where D_α and μ_α are the diffusion coefficient and mobility of the ion type α and $\vec{E_s}$ is the space charge field produced.

Putting $\vec{\Gamma_e} = \vec{\Gamma_i}$ one obtains,

$$- D_i \vec{\nabla} n_i + \mu_i \vec{E_s} = - D_e \vec{\nabla} n_e - \mu_e \vec{E_s}$$

Assuming electron and ion density to be approximately equal i.e. $n_e \simeq n_i = n(z)$ we get for one dimensional case

$$-\frac{D_i}{n}\frac{dn(z)}{dz} + \mu_i E_z = -\frac{D_e}{n}\frac{dn(z)}{dz} - \mu_e E_z \quad (6.6)$$

APPENDIX 6B

Evaluation of the integrals of equation (13)

Formula used

$$\int_0^\infty e^{-Bu^2} u^{2k}\, du = \frac{1.3.\ldots(2k-1)}{2^{k+1}}\sqrt{\frac{\pi}{B^{2k+1}}}$$

(B.6.1)

(i) Since f_{eo} is even function of v,

$\left(\frac{1}{2} m_e v^2\right) v_z$ is the odd function of velocity.

The integral $\iiint_{-\infty}^{+\infty} n_o \left(\frac{1}{2} m_e v^2\right) v_z f_{eo}\, dv_x\, dv_y\, dv_z$ vanishes

(ii) $\iiint_{-\infty}^{+\infty} n_o \left(\frac{1}{2} m_e v^2\right) v_z f'_{e1}\, dv_x\, dv_y\, dv_z$

$$= \frac{n_o m_e}{2}\iiint_{-\infty}^{+\infty}(v_x^2 v_z + v_y^2 v_z + v_z^3)\left(-\frac{v_z}{V_{me}}\right)\frac{\partial f_{eo}}{\partial z}\, dv_x\, dv_y\, dv_z$$

[where $\frac{\partial f_{eo}}{\partial z}$ is given by equation (6.9)]

$$= \frac{n_0 m_e}{2 \nu_{me}} \left(\frac{a}{T_e}\right)^{3/2} \cdot e^{-b/T_e} \cdot \frac{\partial \phi(z)}{\partial z} \iiint_{-\infty}^{+\infty} (v_x^2 v_z^2 + v_y^2 v_z^2 + v_z^4) e^{-Bv^2} dv_x dv_y dv_z$$

$$- \frac{n_0 m_e}{2 \nu_{me}} \phi(z) \iiint_{-\infty}^{+\infty} (v_x^2 v_z^2 + v_y^2 v_z^2 + v_z^4) \frac{\partial}{\partial T_e} \left(\frac{a}{T_e}\right)^{3/2} \cdot e^{-b/T_e} \cdot \frac{\partial T_e}{\partial z} dv_x dv_y dz$$

(B.6.2)

The first part of the R.H.S. of equation (B.6.2) may be written as

$$\text{Const.} \left[\int v_x^2 v_z^2 e^{-Bv^2} dv_x dv_y dv_z + \int v_y^2 v_z^2 e^{-Bv^2} dv_x dv_y dv_z + \int v_z^4 e^{-Bv^2} dv_x dv_y dv_z\right]$$

$$= \text{Const.} \left[\frac{1}{4} \frac{\pi^{3/2}}{B^{7/2}} + \frac{1}{4} \frac{\pi^{3/2}}{B^{7/2}} + \frac{3}{4} \frac{\pi^{3/2}}{B^{7/2}}\right] \text{, using equation (B.6.1)}$$

$$= \text{Const.} \frac{5}{4} \cdot \frac{\pi^{3/2}}{B^{7/2}}$$

$$= -\frac{5}{2} \frac{n_0 k^2 T_e^2}{\nu_{me} m_e} \frac{\partial \phi(z)}{\partial z}$$

Similarly the second part of equation (B.6.1) can be obtained and may be given by

$$-\frac{5}{2} \cdot \frac{n_0 \phi(z) k^2}{m_e \nu_{me}} \cdot T_e \cdot \frac{d T_e}{d z}$$

Hence

$$\iiint_{-\infty}^{+\infty} n_o \left(\frac{1}{2} m v^2\right) f_{e1}' \, dv_x \, dv_y \, dv_z$$

is given by

$$H_1 = -\frac{5}{2} \frac{n_o \phi(z) k^2}{m_e \nu_{me}} T_e \frac{dT_e}{dz} - \frac{5}{2} \frac{n_o}{m_e} \frac{k^2}{\nu_{me}} T_e^2 \frac{d\phi(z)}{dz}$$

$$\text{(iii)} \quad H_2 = \iiint_{-\infty}^{+\infty} n_o \left(\frac{1}{2} m_e v^2\right) f_{e1}'' \, dv_x \, dv_y \, dv_z$$

$$= \frac{e}{\nu_{me} m_e} \cdot \frac{D_e - D_i}{\mu_e + \mu_i} \cdot \frac{1}{\phi(z)} \cdot \frac{d\phi(z)}{dz} \iiint_{-\infty}^{+\infty} n_o \left(\frac{1}{2} m v^2\right) \frac{df_{eo}}{dv_z} \, dv_x \, dv_y \, dv_z$$

using equations (6.8) and (6.12)

$$= \text{const.} \iiint_{-\infty}^{+\infty} v^2 v_z^2 e^{-Bv^2} \, dv_x \, dv_y \, dv_z$$ using equation (6.11)

$$= \text{const.} \ \frac{5}{4} \cdot \frac{\pi^{3/2}}{B^{7/2}}$$

$$= \frac{5}{2} n_o k T_e \mu_e \frac{D_e - D_i}{\mu_e + \mu_i} \cdot \frac{d\phi(z)}{dz}$$

APPENDIX 6.A.C.

Numerical evaluation of the quantity Λ

$$\Lambda = \frac{\int_0^R \frac{F(r)}{r} \, dr}{F(R)}$$

where $F(r) = \int_0^r r\left[1 - \left(\frac{r}{R}\right)^2\right]^n dr$

$$= \frac{R^2}{2(n+1)}\left[1 - \left\{1 - \left(\frac{r}{R}\right)^2\right\}^{n+1}\right]$$

$$F(R) = \frac{R^2}{2n+1}$$

Therefore, $F(r) = F(R)\left[1 - \left\{1 - \left(\frac{r}{R}\right)^2\right\}^{n+1}\right]$

Therefore, $= \Lambda = \frac{\int_0^R \frac{F(r)}{r}\, dr}{F(R)} = \int_0^R \frac{\left[1 - \left\{1 - \left(\frac{r}{R}\right)^2\right\}^{n+1}\right]}{r} dr$

$$= \int_0^R f_r^n\, dr$$

where $f_r^n = \frac{\left[1 - \left\{1 - \left(\frac{r}{R}\right)^2\right\}^{n+1}\right]}{r}$

The integral $\int_0^R f_r^n\, dr$ can be evaluated using

Scarbourgh's method.

Formula used :

$$\Lambda = \frac{R}{15}\left[f_0^{\,n} + f_R^{\,n} + 2\left(f_{2R/5}^{\,n} + f_{4R/5}^{\,n} \right) + 4\left(f_{R/5}^{\,n} + f_{3R/5}^{\,n} \right)\right]$$

The quantities f_0^n, f_R^n, $f_{2R/5}^n$ etc. are obtained numerically from the expression given above for f_r^n and hence Λ's are obtained at different discharge currents. These are given in tabular form in the table 6A-1.

<u>TABLE 6A-1</u>

Discharge current in Amp.	n	f_0^n	$f_{R/5}^n$	$f_{2R/5}^n$	$f_{3R/5}^n$	$f_{4R/5}^n$	f_R^n	Λ
2.3	2.293	0	0.8385	1.4560	1.7111	1.6090	1.3333	.8800
3.1	3.859	0	1.1995	1.9046	1.9681	1.6550	1.3333	1.0561
4.0	3.984	0	1.2273	1.9352	1.9819	1.6564	1.3333	1.0676

REFERENCES

1. Brode, R.B., Rev. Mod. Phys. 5, 257 (1933).
2. Elenbaas, W. The High Pressure Vapour Discharge, North Holland Publishing Co. (1951).
3. Emmons, H.W., Phys. Fluids, 10, 6, 1125 (1967).
4. Emmons, H.W., and Land, R.I., Phys. Fluids, 5, 1489 (1962).
5. Ghosal, S.K., Nandi, G.P. and Sen, S.N., Int. J.Electronics, 44, 4, (1978).
6. Goldstein, L. and Sekiguchi, T., Phys. Rev. 109, 3, 625-30, (1958).
7. Heyaux, Max F., Arc. Phys. Springer Verlag, N.Y. Inc.(1968).
8. Knopp, C.F. and Cambel, A.B., Phys. Fluids, 9, 5, 989-96(1966).
9. Maecker, H., Z. Physik, 158, 392 (1960).
10. Margenau, H. and Adler, F.P., Phys. Rev. 79, 970 (1950).
11. Massey, H.S.W., Burshop, E.H.S., Electronic & Ionic Impact Phenomenon, Vol. 1, 2nd.Edn. p. 29 (1969).
12. Persson, K.B., J. Appl. Phys. 32, 2633 (1961).
13. Ulenbusch, J., Z. Physik, 179, 347 (1964).
14. Von Engel, A., Ionised Gases, Second Edn., Oxford University Press, p. 34 (1964).

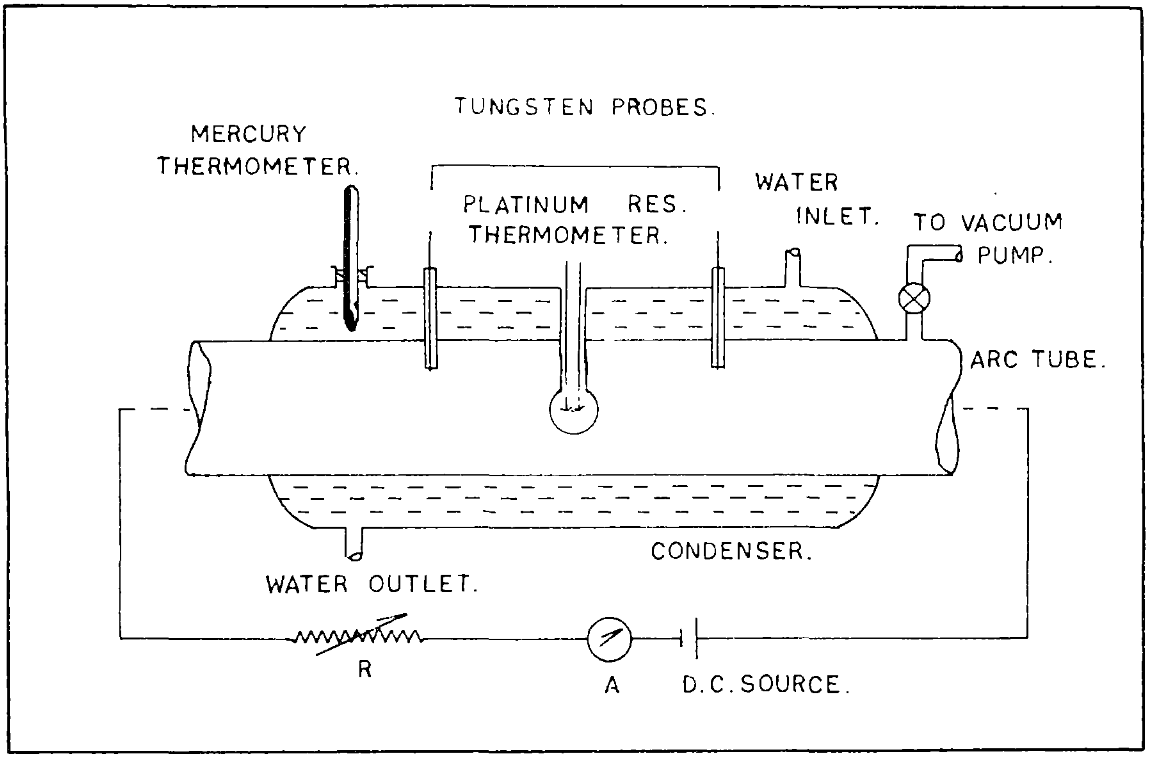

FIG. 6·1. SCHEMATIC EXPERIMENTAL ARRANGEMENT.

INT. J. ELECTRONICS, 1979, VOL. 47, NO. 4, 415–424

Heat flow processes in the positive column of a low pressure mercury arc

S. K. GHOSAL, G. P. NANDI and S. N. SEN

Physics Department, North Bengal University, Darjeeling, India

The problem of heat flow processes within a low pressure mercury arc with water-cooled walls has been investigated utilizing the first-order perturbation technique to Boltzmann transport equation incorporating the term for the observed high gradient of radial distribution of azimuthal electrical conductivity of the arc (Ghosal *et al.* 1978). It is shown that the loss is due to heat conductivity of electrons, ions and neutral particles and also due to ambipolar diffusion by electrons. The experimental results enable us to calculate separately the contribution by the different processes and it is observed that the major part of the heat loss is due to diffusion and the loss due to conduction by electrons, ions and neutral particles is comparatively small. Further from the theory developed and the experimental results obtained, it has been possible to calculate the collision cross-section of electrons with the mercury atoms for electron energies less than 1 eV.

1. Introduction

The heat transport properties of confined electric arc plasma (i.e. the electric arc burning in a tube with cold walls) have been investigated by a number of investigators during the past few decades (Maecker 1960, Ulenbusch 1964, Emmons and Land 1962, etc.); Emmons and Land (1962) measured the thermal conductivity of argon and helium between 5000 K to 10000 K. They assumed Elenbaas–Heller heat balance equation (Elenbaas 1951) with the inclusion of a radiation term. The model, as it has been treated, rests upon an equation expressing simply the balance of three terms:

(1) heat generation by Joule effect;
(2) heat transfer by thermal conduction;
(3) heat transfer by radiation.

However, they were able to show that the radiation loss was a few per cent of the total loss and in their report the radiation effect has been lumped with some effective thermal conductivity. In general, the electrical conductivity assumes a radial distribution within the arc tube but for simplification they assumed the 'channel model' (Hoyaux 1968) for the electrical conductivity distribution within the arc.

In a later paper Emmons (1967) studied the heat transport of high temperature (7500 K to 13 750 K), high pressure argon and helium gas using confined electric arc and tackled the problem very rigorously treating the radiation loss adequately.

Knopp and Cambel (1966) measured the radial temperature distribution within a cylindrically symmetric argon plasma column by spectroscopic method. Using the measured temperature profiles and theoretically calculated radiated power, the thermal conductivity of argon was determined for the temperature range 8500 K to 12 000 K.

Received 25 April 1979; accepted 21 June 1979.

0020-7217/79/4704 0415 $02·00 © 1979 Taylor & Francis Ltd

Most of the experiments aimed at determining the transport properties of noble gases at very high temperatures. At those temperatures thermal ionization prevails and radial distribution of electrical conductivity and thermal conductivity could be calculated using Saha's equation knowing the radial distribution of the gas temperature T. In those cases all the constituents of the gas were considered to be in thermal equilibrium. Goldstein and Sekiguchi (1958) have done elegant experiments employing microwave techniques to determine the thermal conductivity of a decaying glow discharge plasma where the plasma constituents were also in thermal equilibrium.

It is worthwhile to mention at this stage that no reference in the literature is available where the process of heat flow in a confined low pressure arc (where the electrons are far from being in thermal equilibrium with the heavier constituents) has been adequately studied. The present paper proposes to study semi-empirically the heat flow processes occurring within a low pressure mercury arc plasma.

In the previous paper (Ghosal *et al.* 1978) it has been shown that when an arc is formed within a tube, the current density is not uniform throughout the cross-section but is maximum at the axis and minimum at the periphery. This phenomenon gives rise to selective self-heating at the axis of the arc plasma. The arc continuously absorbs power from the source and gives it away to the surroundings. One might therefore be tempted to consider that the mechanism of selective self-heating might be employed to determine the thermal conductivity of the plasma. There are justifications in neglecting the effect of radiation and convection in the case of low temperature arcs but nevertheless it is worthwhile to mention that in this case the process of heat flow requires close observations. In a weakly ionized plasma both the electronic and molecular contributions to thermal conductivity are to be considered. One might predominate substantially over the other depending on the electron temperature, temperature gradients (electron temperature and gas temperature), etc. There might be present another mechanism of heat flow other than thermal conduction, radiation and convection, which arises owing to the fact that electron density distribution within the arc may cause diffusion and energy might be carried away by the electrons. In contrast to the case of high pressure arc this mechanism of heat flow might play a significant role in case of low pressure arcs.

The purpose of the present paper is to present the study of these processes and to compare them in the present experimental conditions. It will also be shown that this study yields valuable information about electron–atom collision cross-section at very low electron energies.

2. Theoretical consideration

In a previous communication (Ghosal *et al.* 1978) the present authors have studied the radial structure of electrical conductivity of a mercury arc plasma in an arc tube by a new radio frequency probe technique. There it has been shown that the radial electrical conductivity distribution function can be well represented by the formula

$$\sigma(r)=\sigma_0\left[1-\left(\frac{r}{R}\right)^2\right]^n \tag{1}$$

where r represents the radial position, R the radius of the tube and σ_0 the conductivity at the axis. The experimentally determined term n is found to be dependent on discharge currents. As indicated in the previous section this radial distribution of electrical conductivity gives rise to a distribution of the rate of heating inside the plasma cylinder defined by the radii r and $r+dr$. The rate of heating per unit length $d\dot{Q}_0$ within the annular space can be represented as

$$d\dot{Q}_0 \alpha f(r)$$

where $f(r)$ is the electrical conductance of the annular plasma cylinder considered and is given by

$$f(r)=2\pi r\, dr\sigma(r)$$

Thus we can write,

$$d\dot{Q}_0 = cr\sigma(r)\, dr$$

where c is a constant. The rate of heating inside the plasma cylinder of radius r is given by

$$\int_0^r cr\sigma(r)\, dr = cF(r) \text{ (say)} \tag{2}$$

Now first considering one dimensional (z) case and assuming that the charged particles are undergoing ambipolar diffusion in the z-direction of the plasma, the steady state perturbed distribution function f_{e1} may be given by the relation

$$v_z \frac{\partial f_{e0}(z, v_x, v_y, v_z)}{\partial z} + \frac{eE_z}{m_e}\frac{\partial f_{e0}}{\partial v_z} = -\nu_{me} f_{e1} \tag{3}$$

where f_{e0} and ν_{me} are the equilibrium distribution function and electron–atom collision frequency respectively and E_z is the field produced in the z-direction due to the diffusion of charged particles. For the present case the equilibrium distribution function (maxwellian) may be given by,

$$f_{e0}(z, v_x, v_y, v_z) = \phi(z)\left(\frac{m_e}{2\pi kT_e}\right)^{3/2} \exp\left(-\frac{m_e v^2}{2kT_e}\right) \tag{4}$$

where $\phi(z)$ is related to the electron density by

$$n(z) = n_0\phi(z) = n_0\left[1-\left(\frac{r}{R}\right)^2\right]^n \tag{5}$$

The field E_z which arrests the tendency of having unequal diffusion speeds for the heavier and lighter charged particle species, may be obtained as

$$E_z = -\frac{1}{\phi(z)}\frac{D_e - D_i}{\mu_e + \mu_i}\cdot\frac{d\phi(z)}{dz} \tag{6}$$

(assuming $n_e \simeq n_i$) where D_e, μ_e, D_i and μ_i are the diffusion coefficients and mobilities of electrons and ions respectively.

The total distribution function $f_e = f_{e0} + f_{e1}$ for electrons undergoing diffusion thus may be obtained using eqns. (3), (4) and (6). Thus one finds the electronic contribution of heat flux by using the relation

$$H_e = \iiint_{-\infty}^{+\infty} n_0\left(\frac{1}{2}m_e v^2\right) v_z f_e \, dv_x dv_y dv_z$$

which is obtained as:

$$H_e = -\frac{5}{2}\frac{n_0\phi(z)k^2}{m_e \nu_{me}} T_e \frac{dT_e}{dz} - \frac{5}{2}\frac{n_0}{m_e}\frac{k^2}{\nu_{me}} T_e^2 \frac{d\phi(z)}{dz} + \frac{5}{2} n_0 k T_e \mu_e \frac{D_e - D_i}{\mu_e + \mu_i}\frac{d\phi(z)}{dz}$$

or,

$$H_e = -K_e \frac{dT_e}{dz} - \frac{5}{2} D_e \frac{d\phi(z)}{dz} n_0 k T_e + \frac{5}{2} n_0 k T_e \mu_e \frac{D_e - D_i}{\mu_e + \mu_i}\frac{d\phi(z)}{dz} \tag{7}$$

where

$$K_e = \frac{5}{2}\frac{n_0\phi(z)k^2}{m_e v_{me}} T_e$$

is the electronic thermal conductivity of plasma, where we have used the relation

$$D_e = \frac{kT_e}{m_e \nu_{me}}$$

Under relevant approximations,

$$\left(\frac{T_e}{m_e} \gg \frac{T_i}{m_i},\ \mu_e \gg \mu_i\right)$$

eqn. (7) can be rewritten as

$$H_e = -K_e \frac{dT_e}{dz} - \frac{5}{2} n_0 k T_e D_A \frac{d\phi(z)}{dz} \tag{8}$$

where $D_A = \mu_i/\mu_e \, D_e$ is the approximate ambipolar diffusion coefficient. The second term of the right-hand side of eqn. (8) can be interpreted in the following way:

The flux of electrons Γ_e executing ambipolar diffusion is given by,

$$\Gamma_e = -D_A \frac{dn(z)}{dz} = -D_A n_0 \frac{d\phi(z)}{dz}$$

Therefore, energy flux carried away by these electrons will be the average kinetic energy multiplied by Γ_e

Again, average kinetic energy $\propto kT_e$.

Thus heat flux will be,

$$H_{\text{amb}} = -\text{constant } kT_e n_0 D_A \frac{d\phi(z)}{dz}$$

Hence, the second term on the right-hand side of eqn. (8) is the heat flux due to the ambipolar diffusion of electrons.

The total heat flux, however, will contain other terms H_i and H_n for the ion species and the neutral particle species respectively. H_i can be neglected in comparison to H_e since ion temperature is very small in comparison to that of electrons.

Thus

$$H = H_e + H_n$$

or

$$H = -\frac{5}{2}\frac{n_0}{m_e}\frac{k^2}{\nu_{me}}\phi(z)T_e\frac{dT_e}{dz} - \frac{5}{2}n_0kT_e\frac{\mu_i}{\mu_e}D_e\frac{d\phi(z)}{dz} - K_n\frac{dT_n}{dz}$$

where K_n is the thermal conductivity for the mercury gas.

Assuming cylindrical symmetry z can be replaced by the radial variable r. Hence

$$H = -\frac{5}{2}\frac{n_0}{m_e}\frac{k^2}{\nu_{me}}\cdot\phi(r)T_e\frac{dT_e}{dr} - \frac{5}{2}n_0kT_e\frac{\mu_i}{\mu_e}D_e\frac{d\phi(r)}{dr} - k_n\frac{dT_n}{dr}$$

The heat flow across the plasma cylinder of unit length of radius r is given by,

$$cF(r) = 2\pi r\left[-\frac{5}{2}\frac{n_0}{m_e}\frac{k^2}{\nu_{me}}\phi(r)T_e\frac{dT_e}{dr} - \frac{5}{2}n_0kT_e\frac{\mu_i}{\mu_e}D_e\frac{d\phi(r)}{dr} - K_n\frac{dT_n}{dr}\right]$$

or, assuming $T_e(r) = \bar{T}_e$ i.e. some suitable average value of electron temperature within the plasma column,

$$c\int_0^R \frac{F(r)dr}{r} = 2\pi\left[\frac{5}{2}\frac{n_0}{m_e}\frac{k^2\phi(r)}{\nu_{me}}\bar{T}_e(T_{e0} - T_{ew}) + \frac{5}{2}n_0k\bar{T}_e\frac{\mu_i}{\mu_e}D_e(\phi_0 - \phi_w) + k_n(T_{n0} - T_{nw})\right] \tag{9}$$

where the suffices 0 and w refer to the values of the relevant quantities at the axis and at the wall respectively. Again, let us turn our attention to eqn. (2),

$$\int_0^R cr\sigma(r)dr = cF(R) = \dot{Q}_0 \text{ (say)}$$

where $\dot{Q}_0$ is the total rate of heating inside the plasma column of unit length. Thus,

$$c = \frac{\dot{Q}_0}{F(R)} \tag{2a}$$

Now using eqn. (2 *a*) we have from eqn. (9)

$$\Lambda\dot{Q}_0 = 2\pi[\alpha\overline{\phi(r)}T_e(T_{e0} - T_{ew}) + \beta(\phi_0 - \phi_w) + k_n(T_{n0} - T_{nw})] \tag{10}$$

(henceforth omitting the bar sign over T_e)
where

$$\Lambda = \int_0^R \frac{F(r)}{r}dr/F(R) \tag{11}$$

with

$$\alpha = \frac{5}{2}\frac{n_0}{m_e}\frac{k^2}{\nu_{me}} \tag{12}$$

and

$$\beta = \frac{5}{2}n_0kT_e\frac{\mu_i}{\mu_e}D_e = \alpha\frac{\mu_i}{\mu_e}T_e^2 \tag{13}$$

The electrical conductivity at the axis of the plasma column is given by the relation,

$$\sigma_0 = \frac{n_0 e^2}{m_e \nu_{me}} \tag{14}$$

Thus,

$$\alpha = \frac{5}{2}\frac{\sigma_0 k^2}{e^2} \tag{15}$$

and

$$\beta = \frac{5}{2}\frac{\sigma_0 k^2}{e^2}\frac{\mu_i}{\mu_e}T_e^2 \tag{16}$$

Assuming $\phi(r) \simeq \frac{1}{2}$ to a first approximation, we can rewrite eqn. (10) in the form

$$\Lambda\dot{Q}_0 = \frac{5}{2}\pi\frac{k^2}{e^2}\sigma_0 T_e(T_{e0} - T_{ew}) + 5\pi\frac{\mu_i}{\mu_e}\frac{k^2}{e^2}T_e^2(\phi_0 - \phi_w)\sigma_0 + 2\pi K_n(T_{n0} - T_{nw}) \tag{17}$$

The quantity $(T_{n0} - T_{nw})$ can be known experimentally by using thermometers (vide experimental arrangement). If the longitudinal electric field of the plasma is assumed to be uniform throughout the cross-section of the plasma the quantity $(T_e - T_n)$ becomes a constant parameter within it.
Thus one can assume

$$T_{e0} - T_{ew} = T_{n0} - T_{nw}$$

Hence eqn. (17) takes the form,

$$\dot{Q}_0 = \frac{5}{2}\pi\frac{k^2}{e^2}\frac{\sigma_0}{\Lambda}T_e(T_{n0} - T_{nw}) + 5\pi\frac{\mu_i}{\mu_e}\frac{k^2}{e^2}\frac{\sigma_0}{\Lambda}T_e^2 + 2\pi\frac{K_n}{\Lambda}(T_{n0} - T_{nw}) \tag{18}$$

where we have put $\phi_0 = 1$ and $\phi_w = 0$ according to the proposed distribution function.

$$\text{The quantity } \Lambda = \frac{\displaystyle\int_0^R \frac{\int_0^r r\sigma(r)dr}{r}dr}{\displaystyle\int_0^R r\sigma(r)dr}$$

can be determined if $\sigma(r)$ is known beforehand.
Equation (18) can also be written as

$$\dot{Q}_0 = \dot{Q}_K + \dot{Q}_D + \dot{Q}_n \tag{19}$$

where

$$\dot{Q}_K = \frac{5}{2}\pi\frac{k^2}{e^2}\frac{\sigma_0}{\Lambda}T_e(T_{n0} - T_{nw}) \tag{20}$$

is the rate of heat flow from the plasma per unit length to the wall due to electronic thermal conductivity,

$$\dot{Q}_D = 5\pi\frac{\mu_i}{\mu_e}\frac{k^2}{e^2}\frac{\sigma_0}{\Lambda}T_e^2 \tag{21}$$

is the heat flow rate due to ambipolar diffusion of electrons; and

$$\dot{Q}_n = 2\pi \frac{K_n}{\Lambda} (T_{n0} - T_{nw}) \tag{22}$$

is the heat flow rate due to thermal conduction of neutral particles.

3. Experimental arrangement and results

The schematic experimental arrangement is shown in the Figure. The apparatus consists of a mercury arc tube (length: 30 cm, internal diameter: 1·5 cm; external diameter: 1·8 cm) with the usual d.c. source, rheostat (R), ammeter (A) arrangements. The arc tube has got some special constructional features. A condenser of length 20 cm is fitted along the mid-portion of the tube to facilitate the flow of water around the positive column of the mercury arc. The temperature of the outflowing water can be measured with an ordinary mercury thermometer fitted with the condenser. A thin glass capsule containing a small platinum-wire coil is placed at the axis of the tube. The coil, having its leads outside the tube, serves as a platinum resistance thermometer. The other accessories which are required to record the resistance of the thermometer at different temperatures are not shown in the Figure.

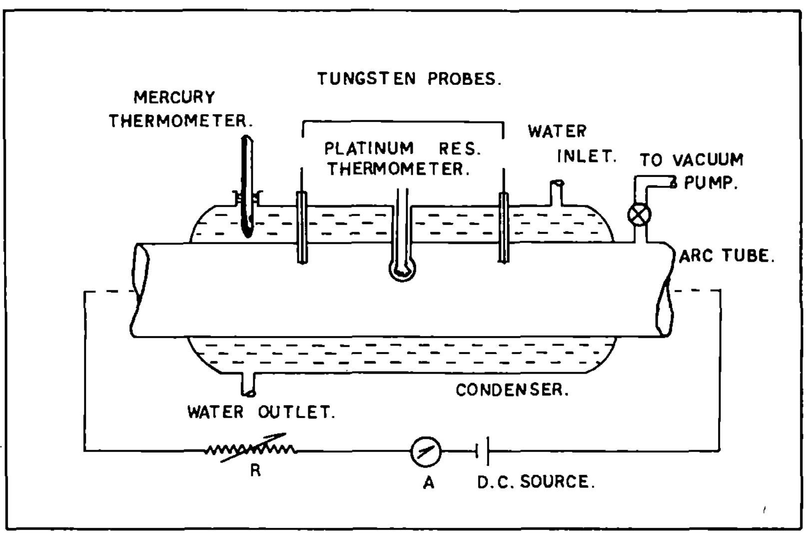

The schematic experimental arrangement.

There is also a double probe arrangement to measure the voltage across the positive column and one of the probes may be utilized to measure the electron temperature.

The experimental procedure is quite straightforward. The platinum resistance thermometer is first calibrated and water is made to flow through the condenser. The arc is then drawn along the tube. Some time is allowed to pass to achieve the thermal equilibrium of the platinum thermometer with the mercury vapour at the axis. The temperature of the platinum thermometer reads T_{n0}, the temperature at the axis. The mercury thermometer reads the temperature θ of the outflowing water. Owing to the finite conductivity of glass, this θ is not the actual peripheral temperature of the plasma. Knowing the thickness and the conductivity (k_g) of glass of the tube, the actual peripheral temperature T_{nw} is calculated. The experiment is repeated for different discharge currents. In each case the rate of supply of heat $\dot{Q}_0$ is calculated by knowing the discharge current and the voltage across the plasma column under study. The experimental results are given below in tabular form (Table 1) which is self-explanatory. The $\dot{Q}_0$s have been calculated from the measured values of E and I.

Table 1.

Discharge current (amperes) (I)	Longitudinal electric field (volt/cm) (E)	$\dot{Q}_0$ in (ergs/cm s)	Temperature at the axis (°C) (T_{n0})	Temperature of the out flowing water (θ) (°C)	Actual gas temperature at the periphery (T_{nw}) (°C)	$T_{n0}-T_{nw}$ (°C)	Electron temperature (probe meas.) (K)	Av. gas temperature $T_n \simeq T_i$ (K)
2·3	0·685	1·57	102·8	37·5	41·3	61·5	$1·76\times10^4$	345·10
3·1	0·472	1·46	105·5	38·0	41·6	63·9	$3·5\times10^3$	346·55
4·0	0·425	1·70	111·4	39·0	43·1	68·3	$3·23\times10^3$	350·30

4. Discussion

In a previous paper (Ghosal *et al.* 1978) the electrical conductivity distribution function was determined for an arc plasma in an arc tube having the same dimension as the present one and the discharge conditions also were the same. Hence here also we assume the same set of distribution functions at 2·3 A, 3·1 A and 4·0 A. of discharge currents. The value of the quantity

$$\Lambda = \frac{\displaystyle\int_0^R \frac{\displaystyle\int_0^r r\sigma(r)dr}{r}\,dr}{\displaystyle\int_0^R r\sigma(r)dr}$$

where $\sigma(r)=\sigma_0[1-(r/R)^2]^n$, the parameter n being dependent on discharge currents, may be solved numerically. Given below in Table 2 the values of σ_0, n and Λ at different discharge currents.

Table 2.

Discharge current (A) (I)	σ_0 (mhos/cm)	n	Λ
2·3	6·26	2·293	0·8800
3·1	18·05	3·859	1·0561
4·0	26·55	3·984	1·0676

In Table 3 the values of quantities $\dot{Q}_0$, $\dot{Q}_K$ and $\dot{Q}_n$ (in joule/cm s.) are inserted for three different discharge currents (2·3 A, 3·1 A and 4·0 A). To obtain $\dot{Q}_n$, the value of k_n has been taken to be $1·5\times10^5$ cal/cm s obtained from the kinetic theory data for

Table 3.

I (A)	$\dot{Q}_0$ (erg/cm s)	$\dot{Q}_K$ (erg/cm s)	$\dot{Q}_D$ (erg/cm s)	$\dot{Q}_n$ (erg/cm s)	$\dot{Q}_K/\dot{Q}_0$	q_e/q_i	T_e (K)	Electron energy (eV)
2·3	1·58	0·45	1·12	$2{\cdot}76\times10^{-2}$	0·28	0·371	$1{\cdot}76\times10^4$	2·97
3·1	1·46	0·22	1·24	$2{\cdot}40\times10^{-2}$	0·15	9·723	$3{\cdot}50\times10^3$	0·45
4·0	1·70	0·32	1·38	$2{\cdot}53\times10^{-2}$	0·19	9·149	$3{\cdot}23\times10^3$	0·42

mercury gas. It may clearly be seen that there is little contribution of $\dot{Q}_n$, i.e. the heat flow due to neutral particles, to the total heat flow rate. It is also observed that heat flow due to electronic thermal conductivity is below 30% of the total flow rate for 2·3 A discharge current and at lower electron temperatures the contribution of electronic thermal conductivity term decreases and in the present situation heat is mainly carried away to the wall by electrons due to ambipolar diffusion. The column for $\dot{Q}_D$ has been obtained from eqn. (19) and $\dot{Q}_n$ has been neglected.

Now eqn. (21) may be utilized to obtain the mobility ratio μ_i/μ_e or expressing this ratio in terms of the mean free path ratio λ_i/λ_e one obtains from eqn. (21)

$$\dot{Q}_D=5\pi\sqrt{\left(\frac{m_e}{m_i}\right)}\frac{k^2}{e^2}\frac{\sigma_0}{\Lambda}\frac{T_e^{5/2}}{T_i^{1/2}}\frac{\lambda_i}{\lambda_e} \tag{23}$$

where T_i is the average ion temperature.

Here we shall make another assumption:

$$T_i \simeq T_n$$

where T_n is the average gas temperature, and so we can rewrite eqn. (23) as

$$\dot{Q}_D=5\pi\sqrt{\left(\frac{m_e}{m_i}\right)}\frac{k^2}{e^2}\frac{\sigma_0}{\Lambda}\frac{T_e^{5/2}}{T_n^{1/2}}\left(\frac{q_e}{q_i}\right)$$

Where q_e/q_i is the ratio of the electron–atom to ion–atom cross-section. In the seventh column of Table 3 the obtained values of q_e/q_i are inserted. Since in the present experiment the ion energy remains fairly constant, we can assume q_i to be a constant quantity. Thus it may be seen that there is a remarkable increase of electron–atom collision cross-section as the electron temperature falls to a value of the order of 3×10^3 K (at discharge currents 3·1 and 4·0 A) from its value $1{\cdot}76\times10^4$ K at 2·3 A discharge current.

In the ninth column the electron energies are inserted in electron volts. The electron–Hg atom collision cross-section can be estimated from Brode's measurements (Brode 1933 and Massey 1969). But for energies <1 eV the q_e values are not well known (Von Engel 1964). However, q_e can be obtained from Brode's curve for electron energy 2·97 eV. This is found to be $6{\cdot}226\times10^{-15}$ cm^2. Utilizing this value of q_e the value of q_i is obtained to be $16{\cdot}78\times150^{-15}$ cm^2. This value shows quite an order of magnitude agreement with the mercury atom-atom collision cross-section, which is $4\pi\sqrt{2}r^2=8{\cdot}059\times10^{-15}$ cm^2, where r is the radius of the mercury atom. This agreement not only justifies our previous arguments but also the obtained value of q_i can be utilized to determine the values of q_e at two different electron energies below

1 eV, thus enabling us to extend Brode's curve in the lower electron energies (Table 4). Our results also corroborate with results obtained by Margenau and Adler (1950) who predicted an occurrence of maxima in the region of lower electron energies from where Brode's measurements begin. The obtained high values of electron–atom collision cross-sections at lower electron energies also explains the sudden fall of electron temperature at higher discharge currents, since as the current is increased the vapour pressure of Hg increases, and thereby lowers the electron energy to some extent. These low energy electrons again suffer greater number of collisions due to a sharp rise of q_e at lower electron energies, thereby lowering the electron energy again and the process continues until the equilibrium is reached.

Table 4.

Discharge current (A)	Electron energy (eV)	q_e (cm^2)
2·3	2·97	$6{\cdot}23\times10^{-15}$
3·1	0·45	$1{\cdot}63\times10^{-13}$
4·0	0·42	$1{\cdot}53\times10^{-13}$

References

BRODE, R. B., 1933, *Rev. mod. Phys.*, **5**, 257.
ELENBAAS, W., 1951, *The High Pressure Vapour Discharge* (Amsterdam: North-Holland).
EMMONS, H. W., 1967, *Physics Fluids*, **10**, 1125.
EMMONS, H. W., and LAND, R. I., 1962, *Physics Fluids*, **5**, 1489.
GHOSAL, S. K., NANDI, G. P., and SEN, S. N., 1978, *Int. J. Electron.*, **44**, 4.
GOLDSTEIN, L. and SEKIGUCHI, T., 1958, *Phys. Rev.*, **109**, 625.
HOYAUX, M. F., 1968, *Arc Physics* (New York: Springer Verlag).
KNOPP, C. F., and CAMBEL, A. B., 1966, *Physics Fluids*, **9**, 989.
MAECKER, H., 1960, *Z. Phys.*, **158**, 392.
MARGENAU, H., and ADLER, F. P., 1950, *Phys. Rev.*, **79**, 970.
MASSEY, H. S. W., and BURSHOP, E. H. S., 1969, *Electronic and Ionic Impact Phenomenon*, Vol. 1, 2nd edition (Oxford University Press), p. 29.
ULENBUSCH, J., 1964, *Z. Phys.*, **179**, 347.
VON ENGEL, A., 1964, *Ionised Gases*, 2nd edition (Oxford University Press), p. 34.